JOURNAL OF GEOPHYSICAL RESEARCH, VOL. 102, NO. B12, PAGES 27,271-27,283, DECEMBER 10, 1997

Paleomagnetism and paleothermometry of the Sydney Basin
1. Thermoviscous and chemical overprinting of the Milton Monzonite

D.J. Dunlop,[1] P.W. Schmidt,[2] Ö. Özdemir,[1] and D.A. Clark[2]

Abstract. The Early Triassic (~245 Ma) Milton Monzonite of the Sydney Basin, Australia, has four distinct components of natural remanent magnetization (NRM) with only slightly overlapping ranges of unblocking temperatures. The low-temperature (LT) component, the first to be thermally demagnetized, is thought to be a Late Cretaceous (≈100 Ma) thermoviscous overprint acquired in slow cooling during uplift. The high-temperature (HT) component, the second to be demagnetized, is probably the primary thermoremanent magnetization (TRM) of the Milton intrusion but could possibly be a Jurassic overprint. LT and HT are usually carried by magnetite and occasionally by pyrrhotite. Samples from nine sites have a further NRM component which unblocks at higher temperatures than HT but below the magnetite Curie temperature of 580°C. This component is argued to be a chemical remanent magnetization (CRM) because of its discrete range of high unblocking temperatures, above those of the thermal components HT and LT, and is called CRM1. CRM1 has almost the same direction as LT and is likely carried by authigenic magnetite produced during uplift ~100 Ma. Samples from five sites have a fourth NRM component, with a direction resembling that of HT but carried by hematite. This fourth component could be a primary TRM but is more likely a CRM and is therefore called CRM2. The HT-CRM2 mean direction is D= 50°, I= 75.5°, defining a paleopole at 16°S, 172°E. The HT-CRM2 paleopole falls near 150 Ma on the Australian apparent polar wander path but is a considerable distance from paleopoles of Permian and Early Triassic age. There is no known tectonic or other remagnetizing event in the Sydney Basin around 150 Ma. For this reason, we propose that the HT-CRM2 paleopole defines a new Triassic segment of the Australian polar wander path. The LT-CRM1 mean direction is D= 348°, I= -79°, with a paleopole falling at 56°S, 158°E, near 100 Ma on the polar wander path. This age is consistent with uplift and cooling related to initial rifting of the Tasman Sea.

1. Introduction

The Milton Monzonite of the Sydney Basin in southeastern Australia has a whole rock K/Ar date of ≈245 Ma (J. R. Richards, as cited by *Joplin* [1968]; *Facer and Carr* [1979]). The intrusion crops out over a 50 km^2 area around the town of Milton in coastal New South Wales, ~175 km SSW of Sydney (Figure 1). It intrudes flat-lying mid-Permian Upper Marine Series sedimentary rocks which have not been significantly tilted during subsidence and subsequent uplift of the Sydney Basin [*Packham*, 1969; *Mayne et al.*, 1974; *Branagan et al.*, 1976]. The Milton Monzonite has been previously studied paleomagnetically by *Schmidt and Embleton* [1981]. Their data were used by *Middleton and Schmidt* [1982] to deduce paleotemperatures reached during basin subsidence, but the paleomagnetically inferred temperatures were anomalously high compared to those estimated from measures of organic diagenesis. This discrepancy was the incentive for our restudy of the Milton Monzonite.

[1]Geophysics Laboratory, Department of Physics, University of Toronto, Toronto, Canada.

[2]Division of Exploration and Mining, CSIRO, North Ryde, New South Wales, Australia.

Paper number 97JB02479.
0148-0227/97/97JB-02479$09.00

The depositional and tectonic history of the Sydney Basin is relatively simple [*Conolly and Ferm*, 1971; *Mayne et al.*, 1974; *Herbert*, 1980]. The basin began to subside in the Early Permian, resulting in deposition of several kilometers of marine sediments. Deposition in the Late Permian and Early Triassic was in marginal to fluvial environments, with numerous coal swamps. The Greta Coal Measures date from this time. Although minor deposition continued into the Jurassic and there was sporadic volcanism and intrusive activity in the Triassic and Jurassic [*Wellman and McDougall*, 1974], the only major tectonic event affecting the entire basin was doming and initial rifting of the Tasman Sea, which caused rapid uplift and erosion 100-70 Myr ago [*Falvey*, 1974].

Rocks presently exposed along the New South Wales coast, the rift margin, are inferred to have reached temperatures of 70-200°C, implying burial to 1-3 km depths if a paleogeothermal gradient of 70°C/km is assumed [*Middleton and Schmidt*, 1982]. The temperature estimates are based on several independent lines of evidence: coal rank and vitrinite reflectance [*Falvey and Middleton*, 1981]; regional laumontite to prehnite metamorphism [*Raam*, 1968]; reset fission track ages in apatites [*Moore et al.*, 1986]; and remagnetization temperatures of natural remanent magnetization (NRM) [*Schmidt and Embleton*, 1981].

The remagnetization temperature T_1 in nature is determined by correcting the maximum unblocking temperature T_{UB} of the burial overprint NRM, measured in relatively rapid laboratory heating, for the effect of much more prolonged heating in nature. *Pullaiah et al.*'s [1975] time-temperature relations for

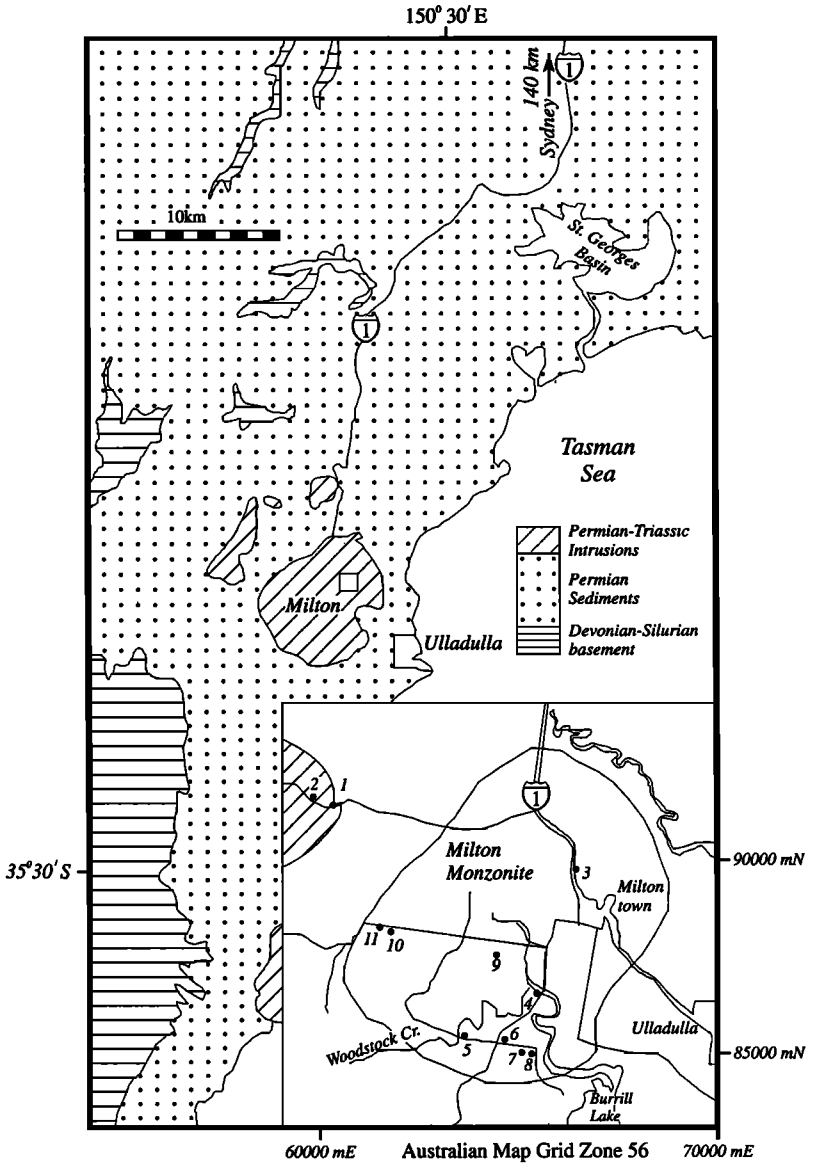

Figure 1. Sampling sites in the Early Triassic Milton Monzonite, near the town of Milton, New South Wales, in the southern Sydney Basin, and geology of the surrounding region.

making this correction, based on *Néel*'s [1949] theory of thermoviscous magnetization in single-domain grains, result in values of T_r that are much higher than those indicated by vitrinite reflectance, metamorphic grade, or fission track annealing. *Middleton and Schmidt* [1982] therefore constructed alternative time-temperature contours using *Walton*'s [1980] relations, which are also based on Néel single-domain theory but which use a different criterion for magnetization unblocking [see *Enkin and Dunlop*, 1988]. The Middleton-Schmidt-Walton contours gave more acceptable estimates of T_r of ~250°C, but these were still significantly higher than average temperatures indicated by vitrinite reflectance.

Middleton and Schmidt [1982] suggested two possible explanations for the discrepancy. (1) Coalification results from temperatures maintained for tens of millions of years, whereas remagnetization might have resulted from a shorter pulse of higher temperature, or (2) multidomain grains, which were detected in the Milton Monzonite, might have different time-temperature relations than single-domain grains. It is important to settle this question because the remagnetization temperature approach to basin analysis is quick, inexpensive, and much more widely applicable than vitrinite reflectance or other measures of organic diagenesis. Other, independent studies on sandstones and limestones in the Hercynian and Appalachian orogens of Europe and North America [*Chamalaun*, 1964; *Kent*, 1985] have also yielded unblocking temperatures that are "anomalously high" (i.e., implying unrealistically high regional T_r values). Thus the remagnetization problem is not limited to a particular lithology, depositional-erosional history, or tectonic setting, and its solution is likely to lie in some general magnetic phenomenon.

With this background in mind, we restudied the Milton Monzonite with a greater areal coverage of sites and more comprehensive thermal treatments than in *Schmidt and Embleton*'s [1981] study. These treatments gave detailed information about the high-temperature thermoremanent magnetization (TRM) and the low-temperature thermoviscous magnetization that overprints it. Thermal demagnetization

also revealed two additional NRM components with still higher unblocking temperatures, whose directions "echo" those of the lower unblocking temperature components. In section 4 we will argue that these two latter components are probably chemical remanent magnetizations (CRMs). Chemical overprinting suggests a third possible explanation of anomalously high unblocking temperatures: the low-temperature NRM component may not be a purely thermoviscous overprint. However, *Dunlop et al.* [this issue] (hereinafter referred to as paper 2) show that multidomain grains can explain the elevated unblocking temperatures that we observe. Chemical overprinting is not required, in this formation at least.

2. Sampling and Measurement Techniques

Schmidt and Embleton [1981] sampled the Milton Monzonite at six sites in two locations. Our 11 sites were distributed more broadly, with a view to examining variations in the composition and domain state of magnetic minerals within the intrusion (Figure 1). Six to eight 2.5-cm-diameter cores, oriented with both sun and magnetic compasses, were drilled at each site, and two or more 2.2-cm-long specimens were cut from each core in the laboratory.

Schmidt and Embleton's [1981] work had shown that the low-temperature and high-temperature components of NRM were cleanly separated by thermal demagnetization but had overlapping coercivity spectra in alternating field demagnetization. We therefore concentrated on thermal demagnetization, which has the added advantage of giving more direct information about remagnetization temperatures. Typically, we demagnetized three specimens of each sample in 23-29 steps to the Curie point of magnetite (580°C), or beyond if significant NRM remained undemagnetized, as was the case at sites 7 and 8. In all, almost 200 individual specimens were stepwise demagnetized.

Because measurements with the SQUID magnetometer were quick, it was possible to operate three large demagnetizing furnaces in tandem, each containing ~20 specimens. While one batch of specimens was being measured, a second batch was being heated to a programmed temperature, and a third batch was cooling, all within remotely controlled field-free spaces. The time required for specimens to reach a uniform temperature throughout their volumes was determined by comparing surface and interior thermocouple readings on dummy samples. This equilibration time was 5-10 min at high temperature. Temperatures were quite uniform within the furnaces, but specimens were nevertheless always returned to the same positions for successive heatings so that the temperature increments would be the same for all specimens.

Even with all economies of scale and the speed permitted by the SQUID magnetometer, ~2 months of measurements were required. The labor invested was repaid by unblocking temperature data of unprecedented quantity and quality, which were indispensable in testing proposed time-temperature relations (see paper 2).

Before thermal treatment, one specimen of most samples was cycled in zero field through the magnetite isotropic temperature T_I around 120 K (low-temperature demagnetization [*Ozima et al.*, 1964]). At T_I, magnetocrystalline anisotropy drops to low values, with the result that domain walls expand and escape from pinning sites. Single-domain remanence, pinned mainly by shape anisotropy, is less affected. Thus low-temperature demagnetization partially erases multidomain NRM, thereby highlighting single-domain NRM. The ratio between the NRM surviving after low-temperature demagnetization to NRM before low-temperature demagnetization is called the memory ratio R.

Low-field susceptibility χ was measured continuously in air, during heating and cooling, between liquid nitrogen temperature (-196°C) and ~620°C for 23 samples, using an automatic recording bridge. Room temperature saturation hysteresis was measured for 35 samples from sites 1-10 using a vibrating-sample magnetometer.

3. Hysteresis and Thermomagnetic Data

At the outset, we should remember that hysteresis and thermomagnetic data characterize the bulk magnetic mineralogy of a rock, but they may be unrepresentative of the phases that carry NRM. Strong-field-induced magnetization (hysteresis) tends to be dominated by large, multidomain grains of magnetite or titanomagnetite. Single-domain or smaller pseudo-single-domain grains of these minerals often carry most of the remanence but contribute relatively little to hysteresis. Minerals like pyrrhotite and hematite are difficult to resolve in hysteresis and also in weak-field-induced magnetization (susceptibility) data for two reasons. They are less magnetic than magnetite, hematite particularly so. Furthermore, they have much larger critical single-domain sizes than magnetite, and therefore tend to contribute less to induced magnetization than to remanence, compared to magnetite of the same grain size.

Site-mean values of reduced saturation remanence M_{rs}/M_s, coercive force $\mu_o H_c$, and Curie temperature T_C, are given in Table 1. The principal magnetic mineral in all samples is magnetite (Fe_3O_4), with T_C ranging from 545 to 580°C. At site 8, samples 8c and 8d had magnetite Curie points (560-580°C) but 8a, 8f, and 8g had $T_C \approx 600$°C, probably indicating cation deficient magnetite, slightly oxidized to maghemite (γFe_2O_3). The Curie point of pure maghemite is ~645°C [*Özdemir and Banerjee*, 1984; *Dunlop and Özdemir*, 1997, pp. 58-60]. We will show later that hematite (αFe_2O_3) is an important NRM carrier, especially at sites 6, 7, and 8, but it is not well expressed in χ-T curves.

Thermomagnetic curves from some sites/ samples (2, 3, 4, 6, 8c, and 8d) are reversible or nearly reversible (Figures 2a, 2b, and 2c), while others (1, 5, 7, 8a, 8f, 8g, 9, 10, and 11) are more complex and irreversible (Figures 2d, 2e, and 2f). Samples 8c and 8d, with $T_C \leq 580$°C, have simple χ-T curves, whereas samples 8a, 8f, and 8g, with $T_C \geq 580$°C, have

Table 1. Hysteresis and Curie Temperature Data

Site	M_{rs}/M_s	$\mu_o H_c$, mT	T_C, °C
1	0.094 ± 0.006	7.2 ± 0.5	555
2	0.069 ± 0.005	5.8 ± 0.4	550
3	0.097 ± 0.015	7.4 ± 0.8	560
4	0.104 ± 0.004	9.6 ± 0.6	550 (545-555)
5	0.106	11.5	548 (545-550)
6	0.146 ± 0.010	12.4 ± 1.2	585
7	0.178 ± 0.006	15.9 ± 1.1	574 (565-580)
8	0.158 ± 0.028	13.4 ± 2.6	588 (560-600)
9	0.107 ± 0.013	9.8 ± 0.8	553 (545-560)
10	0.047 ± 0.004	3.7 ± 0.3	570
11			570

M_{rs}/M_s is saturation remanence normalized to saturation magnetization; $\mu_o H_c$ is bulk coercive force; T_C is Curie temperature (ranges of values in parentheses).

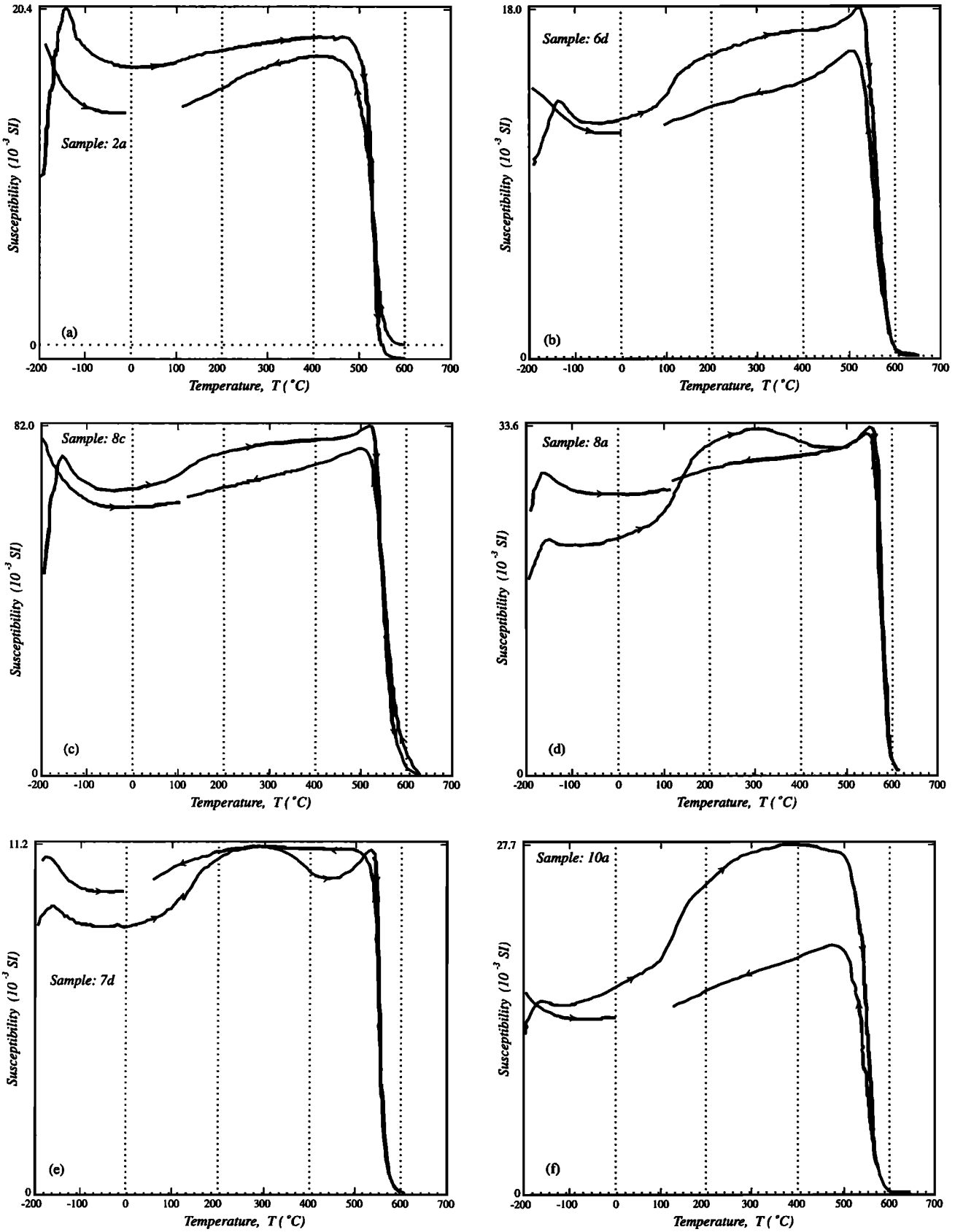

Figure 2. Low-field susceptibility χ as a function of temperature T for selected samples. Initial heating runs started from liquid N_2 temperature (-196°C) and continued to 600-650°C; the sample was then cooled to ~100°C; finally, there was a second heating from -196°C to room temperature or 100°C. All runs were in air. (a)-(c) Relatively simple and roughly reversible behavior in samples from sites 2, 6, and 8. (d)-(f) More complex and irreversible behavior in samples from sites 7, 8, and 10.

complex, irreversible curves. All samples have a pronounced susceptibility peak centered on the magnetite isotropic temperature ($T_I \approx -150°C$), particularly in the initial heating curve, and a similar peak (the Hopkinson peak) just below the magnetite Curie point, with little variation of susceptibility at intermediate temperatures. These are hallmarks of large pseudo-single-domain to multidomain grains of magnetite, in the 20-100 μm size range approximately [e.g., *Clark and Schmidt*, 1982]. Domain wall motion is severely limited by self-demagnetization in these large grains, so that observed susceptibility can only increase significantly when walls are unpinned near T_I or T_C. Single-domain susceptibility is not limited by self-demagnetization and changes over broader temperature ranges (e.g., cooling curve of sample 2a, Figure 2a).

Many of the initial heating curves have an increase in slope around 100°C, which is absent from the cooling curve. This "shoulder" is just resolvable in 8c, more noticeable in 6d, and strongly expressed in 8a and 10a. It might be due to the production of magnetite or maghemite from some less magnetic or nonmagnetic precursor during heating. Sample 7d also has a shoulder in its χ-T curve around 100°C, but it is different from most other samples in that χ decreases markedly between 300 and 400°C (Figure 2e). This broad peak centered on the pyrrhotite Curie point, T_C= 320°C, may be a single-domain Hopkinson peak. However, the thermomagnetic evidence is not compelling. The main evidence for pyrrhotite in site 7 samples comes from thermal demagnetization of their NRMs, described in section 4.

M_{rs}/M_s values for most sites are in the range 0.1-0.15 and $\mu_o H_c$ values range from 7 to 13 mT (Table 1), consistent with moderate to large pseudo-single-domain grains. Values at site 10 are characteristic of ideal multidomain behavior ($M_{rs}/M_s \leq 0.05$, $\mu_o H_c \leq 5$ mT for magnetite [see *Dunlop*, 1969; *Day et al.*, 1977; *Dunlop and Özdemir*, 1997, Chapter 11]. Unusually high values ($M_{rs}/M_s = 0.18$, $\mu_o H_c = 16$ mT) at site 7 may reflect the contribution of single-domain pyrrhotite. A plot of M_{rs}/M_s versus H_c suggests a classification of sites into five groups (Figure 3). Site 10 has the lowest (most multidomain-like) hysteresis parameters, with site 2 somewhat higher. Sites 1, 3, 4, and 9 form a large pseudo-single-domain size grouping, with higher values and a poorer linear correlation between the parameters. Site 5 values fall at the upper end of this grouping but are anomalously high in $\mu_o H_c$. Finally, sites 6, 7, and 8, on the basis of bulk hysteresis alone, appear similar in their linearly correlated, moderate pseudo-single-domain size parameters. Of these trends, only the multidomain character of site 10 samples also turns out to be fully characteristic of the NRM carriers.

4. Thermal Demagnetization Data

Stepwise thermal demagnetization reveals that the NRM of most Milton Monzonite samples comprises four distinct

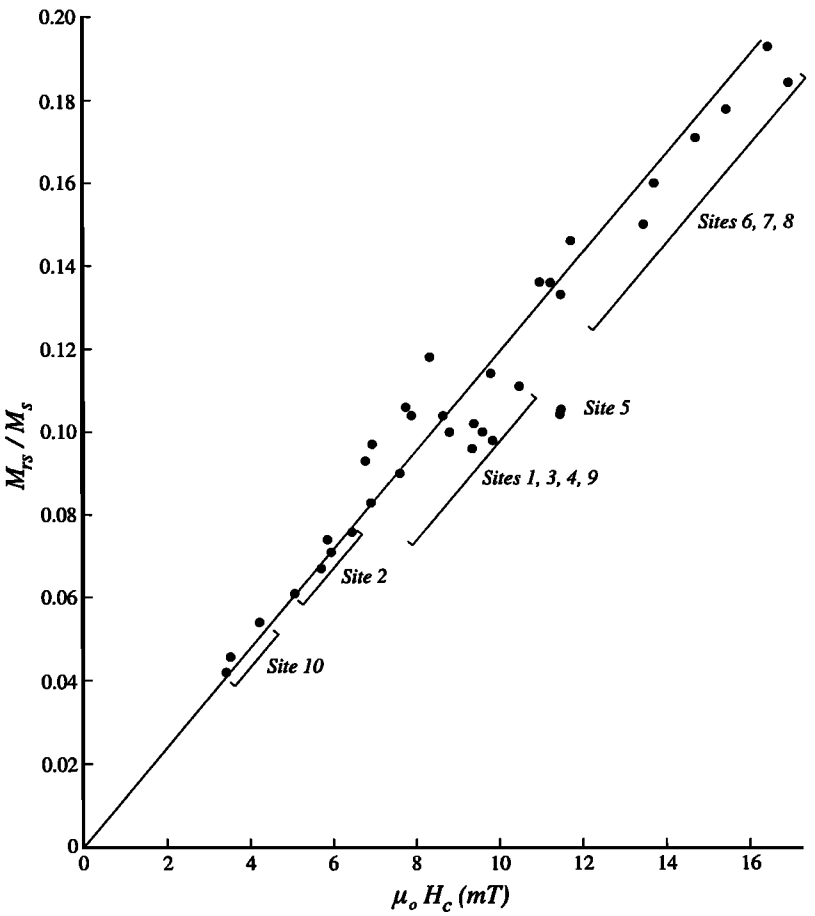

Figure 3. A classification of sites by domain state of the bulk magnetic minerals, based on measurements of the hysteresis parameters M_{rs}/M_s and $\mu_o H_c$. These parameters are approximately linearly correlated, and increasing values of either parameter correspond to decreasing grain size. Only site 10 samples have results characteristic of true multidomain grains of magnetite (≥100 μm approximately).

components (Figures 4 and 5). The first to be demagnetized we will refer to as the low-temperature (LT) component, and the next highest in unblocking temperature T_{UB}, we will call the high-temperature (HT) component. *Schmidt and Embleton* [1981] reported only these two NRM components from thermal demagnetization of their samples, which came from the general locality of our sites 3 and 4 (Figure 1). They interpreted HT to be the primary thermoremanent magnetization (TRM) of the Milton Monzonite and LT to be a viscous partial TRM acquired during uplift and cooling 100-70 Myr ago, i.e., a Late Cretaceous thermoviscous overprint of HT. The LT and HT components are usually carried by magnetite (Figure 4 and Table 2), or occasionally by pyrrhotite (Figure 5; see discussion below).

The two components with the highest unblocking temperatures have directions similar to those of the lower-T_{UB} components. Their high unblocking temperatures are most naturally explained if they are chemical remanent magnetizations (CRMs) or thermochemical remanent magnetizations. We will therefore refer to them as CRM1 and CRM2.

CRM1 is an upward (normal polarity) vector, parallel to LT (Figures 4 and 5) and presumably of similar Late Cretaceous age. CRM1 is usually a small component compared to LT, but occasionally, it is of comparable or even higher intensity (e.g., Figure 5). CRM1 is carried mainly (sites 7, 8) or entirely by magnetite (see maximum T_{UB} values in Table 2), but its unblocking temperatures are higher than those of the HT component, which it overprints. It therefore cannot be a thermoviscous overprint and is probably a CRM.

CRM2 is a small component, carried mainly by hematite. Its T_{UB} values are mostly ≥600°C, and at sites 7 and 8, where CRM2 is most prominent, the unblocking temperatures extend

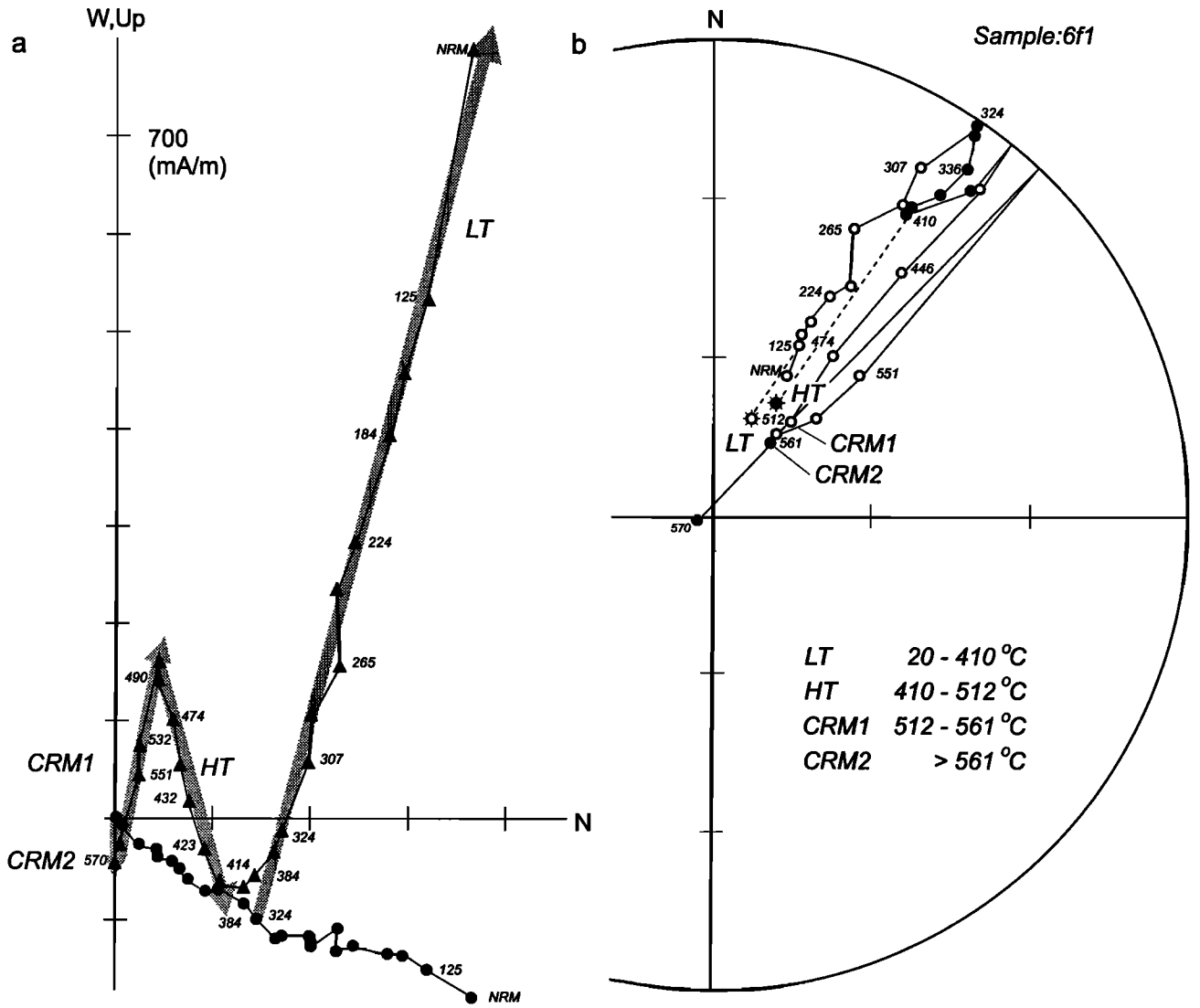

Figure 4. Thermal demagnetization behavior of a typical sample showing four components of NRM: LT, HT, CRM1, and CRM2. The components are revealed (a) by linear segments on orthogonal vector projections (triangles, vertical plane; circles, horizontal plane) and (b) by endpoint or subtracted vector directions in stereographic projections (open, solid circles, upper, lower hemisphere). The LT and HT directions (stars in Figure 4b) are subtracted vectors whose directions correspond to the vectors shown as shaded arrows in Figure 4a. The CRM1 and CRM2 directions also correspond to shaded vectors in Figure 4a and are close to the 512°C and 561°C points, respectively, in Figure 4b. The four NRM components have unblocking temperature (T_{UB}) ranges that are nonoverlapping or nearly so, resulting in relatively sharp junctions between vector projections of the components.

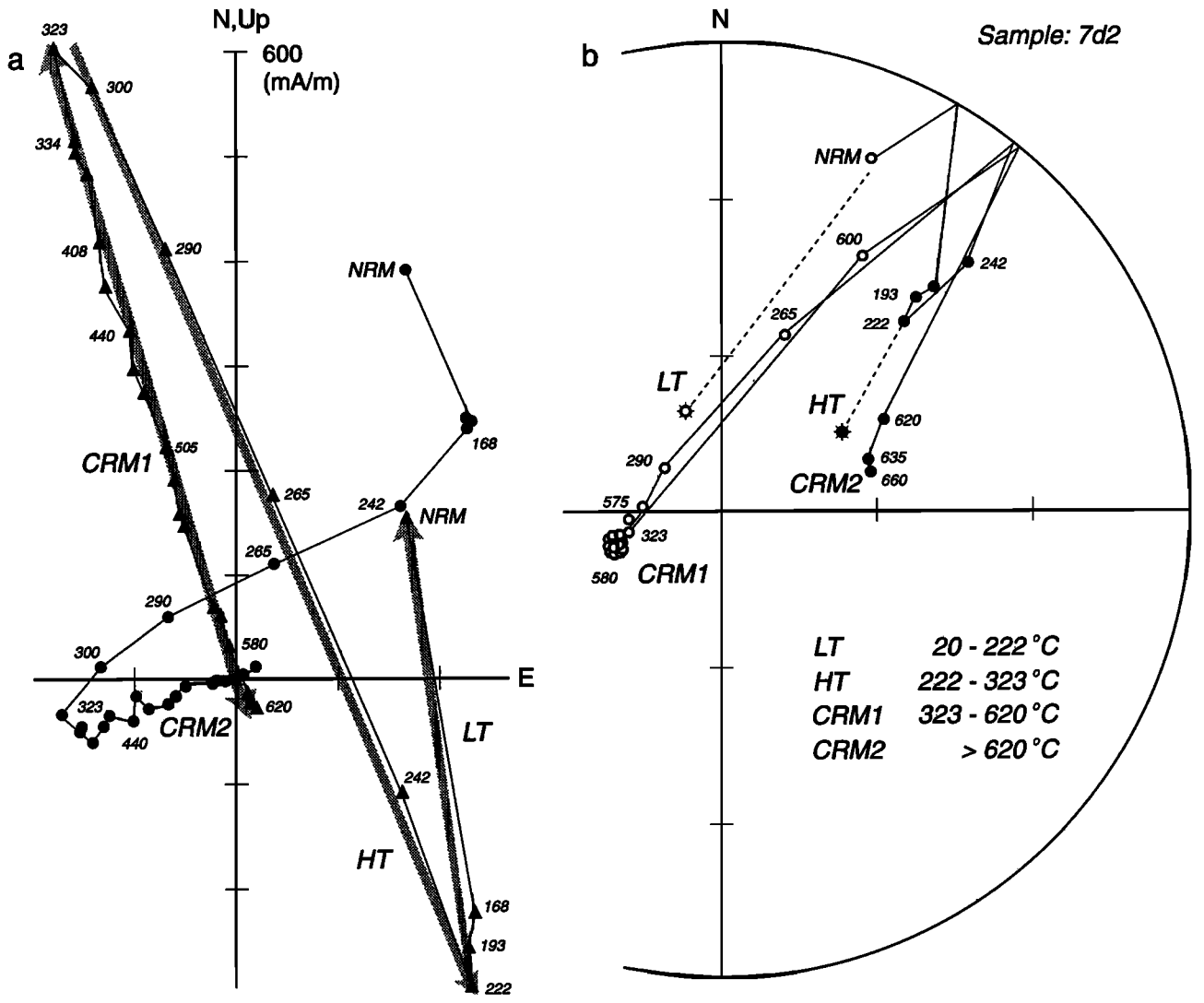

Figure 5. Thermal demagnetization behavior typical of four samples from site 7. The LT and HT components appear to be carried by pyrrhotite (T_C= 320°C) rather than magnetite in these samples. Symbols and projections as in Figure 4.

up to ≈670°C (Table 3 and Figure 6). CRM2 is a downward (reverse polarity) vector, approximately parallel to HT. It could be part of the primary TRM, the hematite counterpart to HT, but we consider it more likely that CRM2 is a Triassic age CRM.

Four samples from site 7 behave in the manner shown in Figure 5. Four NRM components are present but LT has maximum unblocking temperatures of ~220°C (Table 2) and HT has a maximum T_{UB} of ~310°C (Table 3). Our interpretation is that HT is a Triassic age NRM carried by pyrrhotite (T_C= 320°C), and LT is a Late Cretaceous thermoviscous overprint, also in pyrrhotite. The usual magnetite HT component is completely absent in these samples. However, magnetite with the unblocking temperature range typical of the HT component in other samples carries CRM1, echoing the LT direction.

CRM1 is found at all sites except sites 10 and 11, although only at sites 6, 7, and 8 was it large enough to permit reliable estimates of its mean direction (Table 2). CRM2 is found at sites 3, 4, 6, 7, and 8 and is large enough at the latter two sites to give a reliable mean direction (Table 3). It is interesting that both CRM1 and CRM2 occur at sites 3 and 4, where *Schmidt and Embleton* [1981] sampled, but their presence was only revealed by the very detailed thermal demagnetization undertaken in the present study. A similar situation in the Mauch Chunk Formation of Pennsylvania was described by *Kent and Opdyke* [1985].

It is also interesting that chemical overprinting, hitherto unsuspected, is so widespread in the Milton Monzonite. There are again parallels with North American rocks of the Appalachians and adjacent midcontinent [*McCabe and Elmore*, 1989]. About half the Milton sites bear a Triassic hematite NRM, probably a CRM, while almost all sites have a magnetite CRM of essentially the same age as LT, the uplift viscous partial TRM. At site 7, CRM1 is sometimes larger than LT (Figure 5). The question arises: Is LT really a thermoviscous overprint of HT or is it too a CRM, in whole or in part?

Figure 6 shows total intensity decay curves for the separate components, constructed from the thermal demagnetization data of Figures 4 and 5. All components have remarkably linear decay curves, unlike the usual thermally discrete curves in which decay is concentrated just below the Curie point of

Table 2. LT and CRM1 Paleomagnetic Data After Thermal Demagnetization

Site	Location	N	N'	D, deg	I, deg	k	α_{95}, deg	$(T_{UB})_{max}$, °C	n
				LT Component Data[a]					
1	603/914	6	6	1	-58	89	7	401 ± 35	11
2	596/915	6	2	238	-78	684		333 ± 15	12
3	663/846	7	7	14	-78	258	4	395 ± 18	14
4	656/866	8	8	12	-79	91	6	428 ± 22	15
5	634/854	6	5	324	-79	104	8	440 ± 15	16
6	646/853	6	6	9	-75	203	5	394 ± 27	12
7	651/851	7	7	3	-70	86	7	220 ± 12	15
8	652/851	7	5	10	-64	49	11	267 ± 61	14
9	644/875	6	4	346	-78	75	11	427 ± 6	6
(10	620/883	6	6	22	-15	122	6	516 ± 14	12)
11	617/884	6	4	241	-75	22	20	538 ± 8	8
LT mean			10	350.5	-77.5	35	8		
				CRM1 Component Data[b]					
1								551 - 570	9
2								555 - 577	7
3								568 ± 6	14
4								571 ± 5	16
5								~575	2
6		6	6	25	-79	97	7	570 ± 5	18
7		7	7	304	-81	101	6	604 ± 16	16
8		7	5	298	-83	143	6	600 ± 6	17
9								570	3
CRM1 mean			3	334.6	-83.3	121	11		
Combined mean[c]			13	348.3	-79.0	42	6.5		

Site locations are grid references for Australian Map Grid Zone 56 (see Figure 1). For example, 603/914 (site 1) is an abbreviation for 260300 m E, 6091400 m N, i.e., the references omit the first one or two digits (which are obvious from the map location of Milton) and are accurate to the nearest 100 m. N, N' are number of samples taken and number used in averaging at each site, respectively. D and I are declination and inclination of NRM after cleaning; k is Fisher precision; α_{95} is the radius of the 95% cone of confidence about the mean direction. $(T_{UB})_{max}$ is the maximum unblocking temperature of each component, determined from vector diagrams (e.g., Figures 4 and 5) and averaging n specimen results per site. The semiaxes of the oval of 95% confidence about the paleopole are dp and dm.

[a]Paleopole for LT component is 157.8°E, 58.7°S, with dp=14.0° and dm=15.0°.

[b]Paleopole for CRM1 component is 158.7°E, 47.0°S, with dp=21.1° and dm=21.6°.

[c]Combined paleopole is 158.0°E, 55.9°S, with dp=11.7° and dm=12.3°.

each magnetic phase. A very broad size spectrum of magnetic carriers (mainly magnetite) is one possible explanation. However, the bulk hysteresis and thermomagnetic properties favored moderate to large pseudo-single-domain grains, in some cases approaching ideal multidomain size. Multidomain and large pseudo-single-domain grains have much more linear thermal decays of TRM and partial TRM than most single-domain grain assemblages [*Bol'shakov and Shcherbakova*, 1979; *Xu and Dunlop*, 1994; *Dunlop and Özdemir*, 1997, Figures 10.11, 16.11] and can also explain the observed decays.

More germane to the question posed earlier is the wide separation of the T_{UB} ranges of the LT and CRM1 components. In samples 7d-f, there is an ~100°C window, and in other samples there is often an even wider window, between the two, occupied by HT unblocking temperatures. If LT were even in part a CRM similar in origin to CRM1, it would inevitably have attacked and overprinted HT in this intermediate T_{UB} interval. The sharp separation of LT and HT unblocking temperatures (discussed in detail in paper 2) is compelling evidence that LT is a thermoviscous, not a chemical, overprint.

5. Paleomagnetic Data

Site-mean cleaned NRM directions, Fisher statistics k and α_{95}, and maximum unblocking temperatures for each of the four components are summarized in Tables 2 and 3. The site 10 LT directions are anomalously shallow and have been omitted from averaging to obtain the LT mean. Four of the six samples from site 2 also had shallow inclinations, in this case streaked along a great circle between LT and HT directions, and were omitted in averaging. Site-mean and grand-mean directions for LT, CRM1, and HT are plotted in Figure 7.

LT and CRM1 are of normal polarity (as expected for the Cretaceous normal superchron (118-83 Ma): see section 6) and have mean directions that are indistinguishable at the 95% confidence level. The combined LT-CRM1 grand mean direction is D=348.3°, I= -79.0° (k= 42, α_{95}= 6.5°), in exact agreement with *Schmidt and Embleton*'s [1981] result, D= 348°, I= -79°. The grand mean is distinctly different from the present Earth's field direction but is similar to directions for dated Late Cretaceous units. The corresponding (south) paleopole position is 56°S, 158°E (dp= dm= 12°), falling around 100 Ma on the Australian apparent polar wander path (Figure 8).

Table 3. HT and CRM2 Paleomagnetic Data After Thermal Demagnetization

Site	N	N'	D, deg	I, deg	k	α_{95}, deg	$(T_{UB})_{max}$, °C	n
				HT Component Data[a]				
1	6	6	22	+62	79	8	538 ± 18	15
2	6	6	88	+77	186	5	547 ± 19	18
3	7	7	43	+70	42	10	534 ± 33	18
4	8	8	50	+72	40	9	544 ± 15	18
5	6	5	59	+80	242	5	541 ± 10	16
6	6	6	29	+68	244	4	503 ± 15	18
7	7	6	60	+70	81	8	309 ± 10	12
							508 ± 17	6
8	7	5	45	+74	45	12	475 ± 20	11
9	6	6	34	+73	101	7	542 ± 8	5
11	6	2	133	+80	>10^3		~575	3
HT mean		10	47.4	+74.4	71	6		
				CRM2 Component Data[b]				
3							>577	7
4							>577	2
6							>580	18
7	7	6	64	+79	55	9	665 ± 9	13
8	7	6	79	+82	158	5	672 ± 5	15
CRM2 mean		2	70.2	+80.6	890			
Combined mean[c]		12	49.9	+75.5	77	5		

Symbols are the same as in Table 2.

[a]Paleopole for HT component is 172.1°E, 13.6°S, with dp=9.9° and dm=10.9°.

[b]Paleopole for CRM2 component is 169.9°E, 27.5°S.

[c]Combined paleopole is 171.8°E, 15.8°S, with dp=8.4° and dm=9.2°.

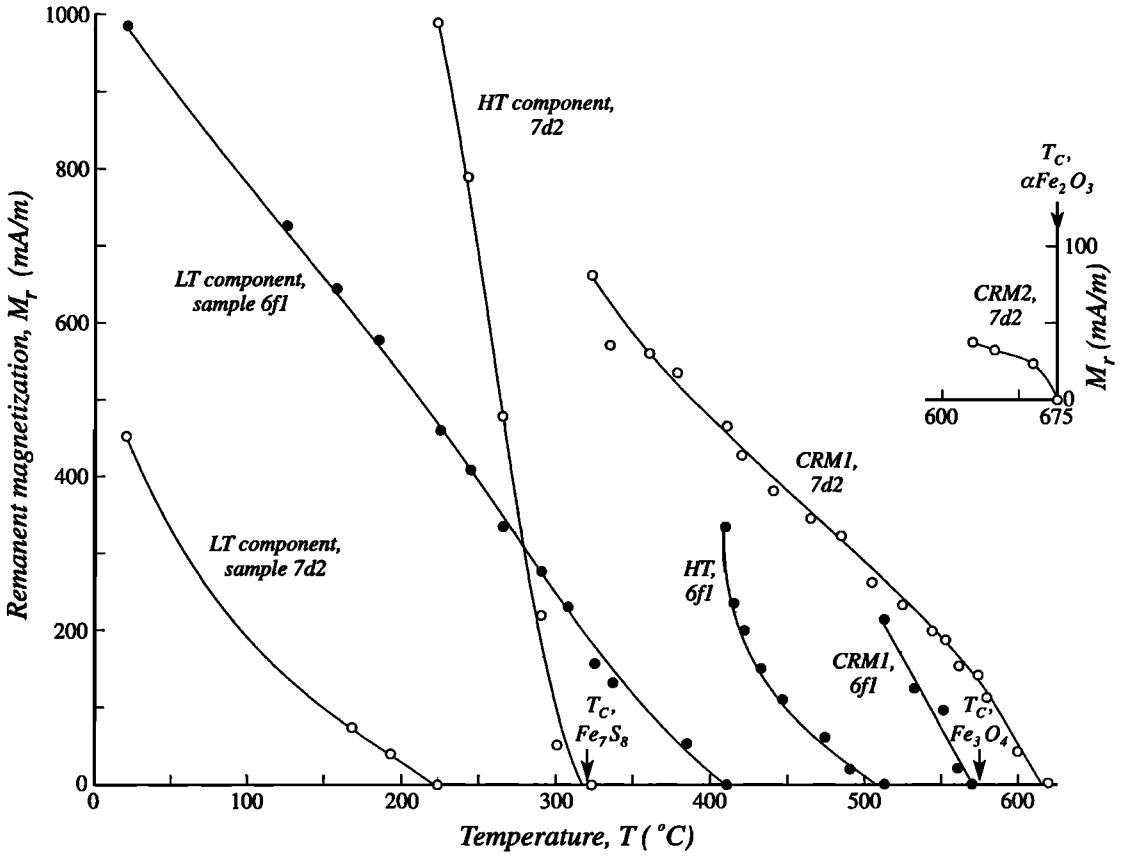

Figure 6. Thermal demagnetization intensity decay curves plotted separately for each of the four components in samples 6f1 and 7d2 (determined from the orthogonal vector projections of Figures 4 and 5). The decay curves are almost linear ("thermally distributed") rather than "thermally discrete." Note the enlarged scale for CRM2.

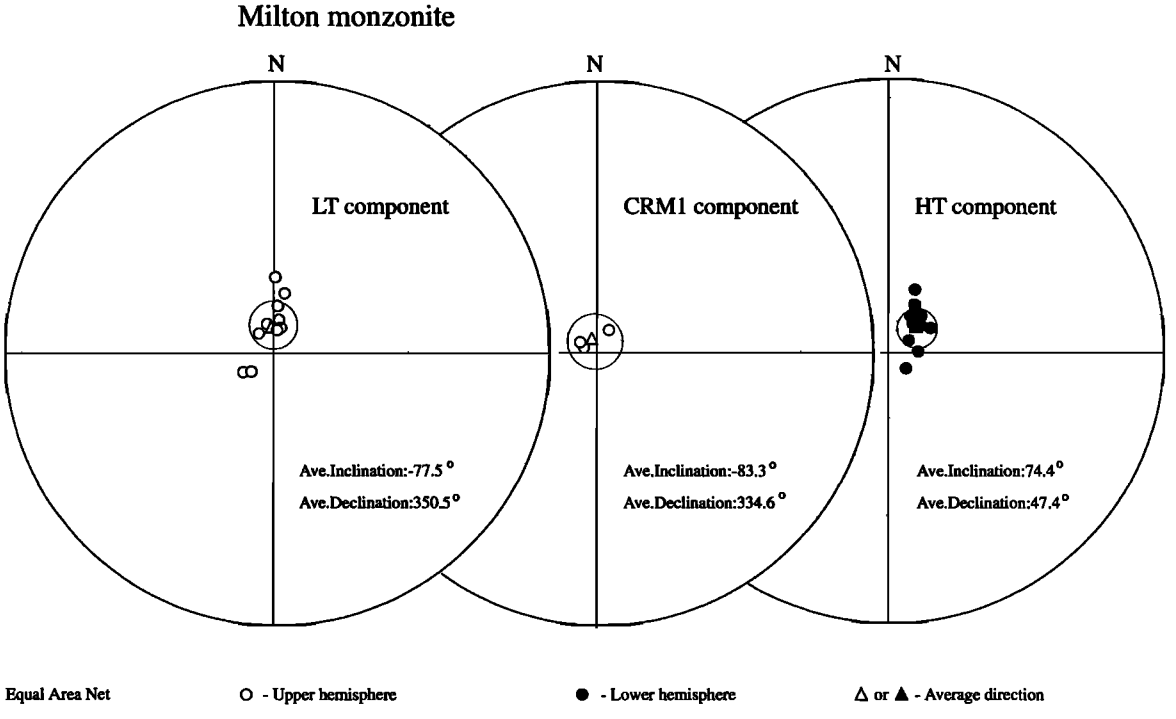

Figure 7. Site-mean cleaned paleomagnetic directions for the LT, CRM1, and HT NRM components of the Milton Monzonite. Triangles and enclosing circles denote grand means and circles of 95% confidence for each component.

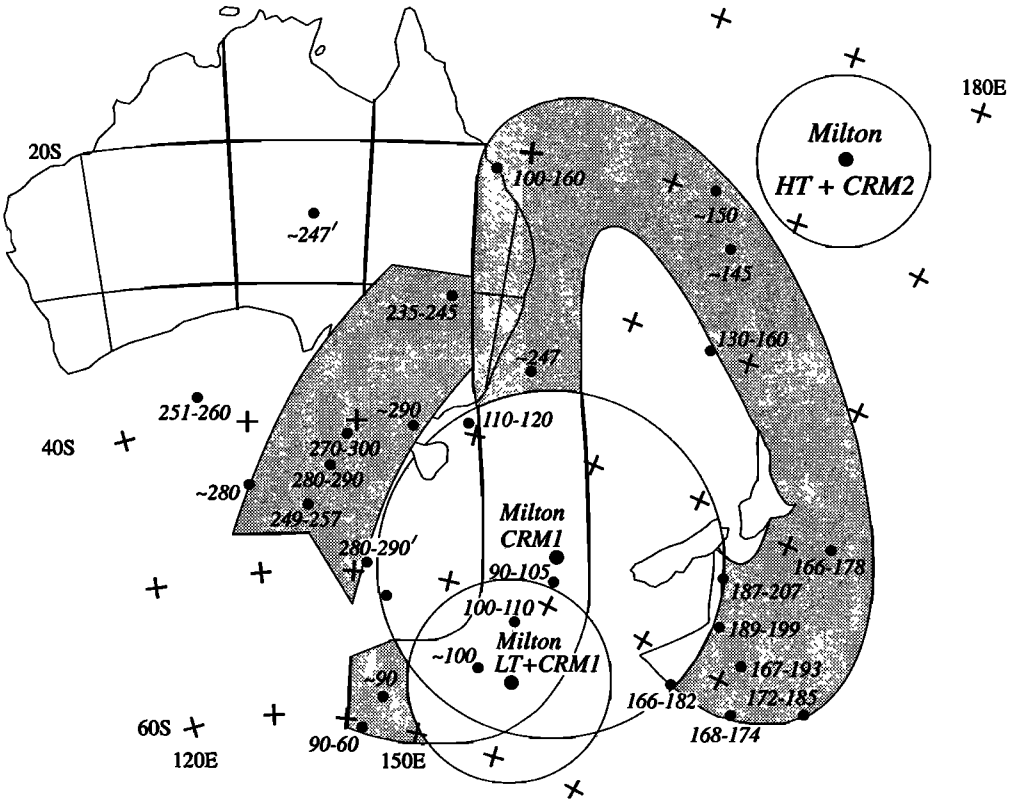

Figure 8. Permian to mid-Cretaceous apparent polar wander path for Australia. Numbers on paleopoles are ages in Ma; individual paleopoles are listed in Table 4. Paleopoles and approximate ovals of confidence for LT+CRM1, CRM1, and HT+CRM2 are indicated. Note that HT+CRM2 and LT+CRM1 have nonintersecting ovals and cannot be of similar ages.

HT and CRM2 are of reverse polarity and have similar directions. The CRM2 mean falls just outside the 95% circle of confidence for HT, but since CRM2 has low intensity compared to LT, HT, or even CRM1 (compare Figure 6) and is measurable with confidence at only two sites, it is probably not greatly different in direction or time of acquisition from HT. The combined HT-CRM2 mean, using HT data from all 11 sites and CRM2 from only 2 sites, is D= 49.9°, I= 75.5° (k= 77, α_{95}= 5°), which is indistinguishable from *Schmidt and Embleton*'s [1981] result, D= 60°, I= 78°. The corresponding (south) paleopole position, 16°S, 172°E (dp=8°, dm=9°), falls around 150 Ma on the Australian apparent polar wander path (Figure 8) and is rather far removed from Permian and Early Triassic paleopoles for eastern Australia (poles ranging from 280-290 Ma to 235-245 Ma in age in Figure 8). The discrepancy cannot be explained by tilting because the Milton Monzonite intrudes flat-lying strata, as noted in the Introduction.

One possibility is that the whole rock K/Ar date of 245 Ma for the Milton Monzonite is slightly older than its true age. Most of the paleopoles in Figure 8 and Table 4 are for extrusive or shallow intrusive rocks, but the Milton Monzonite is a hypabyssal intrusion that may contain some excess argon. Judging by the HT+CRM2 paleopole position, a Late Triassic age of ~220-230 Ma for the Milton HT magnetization would be plausible. A loop joining the Permian and Early Triassic paleopole group (near southeastern Australia in Figure 8) to the Early to Middle Jurassic group (~165-200 Ma, south of New Zealand) could then incorporate the Milton HT+CRM2 paleopole in the apparent polar wander path. This hypothetical loop is of about the same length as the subsequent "Coral Sea loop" linking the ~170 Ma Middle Jurassic poles to the ~100 Ma Cretaceous poles. The overall picture would then be of quasi-static apparent polar wander during the Permian and Early Triassic and again during the Early and Middle Jurassic with 40-60 Myr long periods of more rapid plate motion following each standstill.

6. Discussion

We have confirmed earlier determinations of the HT and LT mean directions for the Milton Monzonite and in addition have discovered these same directions echoed in high unblocking temperature magnetite and hematite overprints, CRM1 and CRM2. In each case, the CRM has steeper inclination than the TRM or pTRM it resembles. The differences in directions are not statistically significant, but they may reflect slight differences in the time of remanence acquisition between HT and CRM2 and between LT and CRM1. For this reason, we propose that CRM2 is likely a CRM acquired by authigenic hematite and therefore slightly younger than HT, rather than a TRM in primary hematite.

CRM1 is carried by authigenic magnetite, probably a product of hydrothermal alteration. There are two possibilities. CRM1 could be the result of deep penetration by hydrothermal solutions during heating, doming and initial rifting over a rising plume prior to full rifting and spreading of the Tasman Sea (~80 Ma). In this case, CRM1 would be somewhat older than LT, which was produced by slow cooling in a later stage of uplift. Alternatively, CRM1 could be the product

Table 4. Australian Paleopoles of Permian to Cretaceous Age

Age, Ma	Formation	Reference	Database
~290	Featherbed Volcanics D	*Klootwijk et al.* [1993]	
280-290	Mount Leyshon	*Clark* [1996a]	
280-290′	Tuckers Range	*Clark* [1996b]	
~280	Featherbed Volcanics A	*Klootwijk et al.* [1993]	
270-300	Bulgonunna Volcanics	*Lackie et al.* [1992]	
251-260	Newcastle Coal Measures	H. Théveniaut (personal communication, 1996)	
249-257	Gerringong Volcanics	*Irving and Parry* [1963]	995
~247	Dundee Ignimbrite	*Lackie* [1989a]	
~247′	Dundee Rhyodacite	*Lackie* [1989b]	2566
235-245	Patonga Claystone	*Embleton and McDonnell* [1980]	1610
220-230?	Milton Monzonite HT+CRM2	this paper	
189-199	Western Victoria Basalt	*Schmidt* [1976a]	781
187-207	Garawilla Volcanics	*Schmidt* [1976b]	780
172-185	Jurassic Intrusives	*Schmidt* [1976b]	780
168-174	Barrenjoey Dyke	*Robertson* [1979]	1239
167-193	Jurassic compilation	*Embleton* [1981]	
166-182	Tasmanian Dolerites	*Schmidt and McDougall* [1977]	1113
166-178	Kangaroo Island Basalt	*Schmidt* [1976a]	781
130-160	Hornsby Breccia	*Schmidt and Embleton* [1981]	1238
~150	Bendigo Dykes	*Schmidt* [1976a]	
~145	Late J-Early K compilation	*Embleton* [1981]	
100-160	Erskine Park Sill	*Robertson* [1979]	1239
110-120	Otway Formation	*Idnurm* [1985]	1201
100-110	Cygnet Alkaline Complex	*Robertson and Hastie* [1962]	974
~100	Mount Dromedary	*Schmidt* [1976c]	
≈100	Milton Monzonite LT+CRM1	this paper	
90-105	Bunbury Basalt	*Schmidt* [1976a]	781
~90	Patonga Claystone overprint	*Embleton and McDonnell* [1980]	1238
90-60	Hornsby Breccia overprint	*Schmidt and Embleton* [1981]	1238

Database number is the Global Paleomagnetic Database reference number [*McElhinny and Lock*, 1996].

of low-temperature hydrothermal alteration late in uplift, after the LT magnetization had been blocked by cooling. The paleopole position for CRM1 alone, 47°S, 159°E, falls in an older position along the polar wander path than LT or LT+CRM1 (Figure 8), favoring the former scenario.

The HT-CRM2 paleopole is puzzling. It does not match Late Permian and Early Triassic poles from Australia but lies close to 150 Ma on the Coral Sea loop of the Australian apparent polar wander path. Around 150 Ma, the Sydney Basin was tectonically quiescent. Basin subsidence and deposition had ceased by the Early Jurassic (~200 Ma) and uplift did not begin until 100 Ma at the earliest. The reverse polarity of HT and CRM2 is also somewhat unexpected because 150 Ma was a time of predominantly normal polarity, although not exclusively so. Late Jurassic remagnetization therefore seems unlikely, although it cannot be ruled out.

A magnetization age for HT and CRM2 significantly younger than 150 Ma can be ruled out on both rock magnetic and paleomagnetic grounds. If HT and CRM2 are younger CRMs, their probable age is no older than ~100 Ma, the time of doming and initiation of marginal rifting seaward of the Sydney Basin. They would therefore be expected to have similar directions to LT and CRM1 and normal, not reverse, polarity. The Milton samples contain a mixture of magnetic phases, principally magnetite, hematite, and pyrrhotite (Figure 2). Self-reversal in one of these phases is conceivable, but in both magnetite (HT) and hematite (CRM2) it is highly unlikely. Furthermore, the HT-CRM2 direction is not antipodal to the LT-CRM1 direction (e.g., Figures 4 and 7). If either the LT or HT group of directions in Figure 7 is reversed and compared to the other, the grand means and circles of confidence are distinct by a large angle. Equivalently, the ovals of confidence about the LT-CRM1 and HT-CRM2 paleopoles in Figure 8 are nonintersecting by a large angle. HT-CRM2 is therefore not similar in age to LT-CRM1.

Since it is unlikely that HT and CRM2 are either Late Jurassic or Cretaceous remagnetizations, we prefer the hypothesis advanced earlier. We assume that the Milton Monzonite is of Late Triassic age (~230-220 Ma), rather than Early Triassic as indicated by its 245 Ma K/Ar date, and that HT is the primary TRM dating from initial cooling of the intrusion. CRM2 is thought to be a slightly younger hematite CRM. The HT-CRM2 paleopole defines a new loop (~240-200 Ma) in the Australian apparent polar wander path, linking Permian/Early Triassic poles to Early/Middle Jurassic poles. This loop crosses the younger Coral Sea loop (~165-100 Ma) around 150 Ma, producing the ambiguity in magnetization age of HT-CRM2.

7. Conclusions

1. The predominant magnetic mineral in the Milton Monzonite is magnetite with T_C = 545-580°C. Hematite and pyrrhotite also carry NRM but are not well expressed in susceptibility and hysteresis.

2. The magnetite detected by bulk hysteresis measurements is of moderate to large pseudo-single-domain size (≥10 μm), approaching true multidomain size (≥100 μm) at site 10.

3. The NRM of the Milton Monzonite consists of four distinct magnetizations, low temperature (LT), high temperature (HT), and magnetite and hematite CRMs (CRM1 and CRM2), with nonoverlapping or only slightly overlapping ranges of unblocking temperatures.

4. The HT and LT components are believed to be of thermal origin. HT is the primary (Triassic) TRM. LT is a Middle to Late Cretaceous thermoviscous overprint acquired in slow cooling during uplift. HT and LT are carried by magnetite in most samples and by pyrrhotite in four samples from site 7.

5. CRM1 is carried by authigenic magnetite produced during uplift around 100 Ma. It is similar in direction to LT but may be slightly older.

6. CRM2 is similar in direction to HT. It could be a primary hematite TRM but is more likely a CRM slightly younger than HT.

7. The HT-CRM2 mean direction is D= 50°, I= 75.5°, similar to that found by *Schmidt and Embleton* [1981]. The paleopole falls at 16°S, 172°E, near 150 Ma on the Australian apparent polar wander path but a considerable distance from Permian and Early Triassic poles from Australia. There is no known tectonic or other magnetizing event in the Sydney Basin around 150 Ma, and so the HT-CRM2 pole probably lies on a new Middle Triassic to Early Jurassic segment of the polar wander path.

8. The LT-CRM1 mean direction is D= 348°, I= -79°, identical to that found by *Schmidt and Embleton* [1981]. The paleopole falls at 56°S, 158°E, near 100 Ma on the Australian apparent polar wander path. This age is consistent with uplift and cooling related to initial rifting of the Tasman Sea.

Acknowledgments. Most of the paleomagnetic research was done while D.J.D. and Ö.Ö. were Visiting Scientists at CSIRO. We thank Mark Huddleston for thermomagnetic measurements and Jeff Wood for hysteresis determinations. Helpful reviews and suggestions by Gillian Turner, Bob Butler, and an anonymous referee greatly improved the paper. The analysis and interpretation phases of the work were supported by NSERC research grant A7709 to D.J.D.

References

Bol'shakov, A. S., and V. V. Shcherbakova, A thermomagnetic criterion for determining the domain structure of ferrimagnetics, *Izv. Phys. Solid Earth, Engl. Transl., 15*, 111-117, 1979.

Branagan, D. F., C. Herbert, and T. Langford-Smith, *An Outline of the Geology and Geomorphology of the Sydney Basin*, 60 pp., University of Sydney, Sydney, Australia, 1976.

Chamalaun, F. H., Origin of the secondary magnetization of the Old Red Sandstone of the Anglo-Welsh cuvette, *J. Geophys. Res., 69*, 4327-4337, 1964.

Clark, D. A., New Permian, Devonian and Silurian poles from the Charters Towers Province - Implications for the Palaeozoic APWP of Gondwana (abstract), *Eos Trans. AGU, 77(22)*, West. Pac. Geophys. Meet. Suppl., W19, 1996a.

Clark, D. A., Palaeomagnetism of the Mount Leyshon Intrusive Complex, the Tuckers Igneous Complex and the Ravenswood Batholith, *CSIRO Explor. Min. Rep. 318R*, 1996b.

Clark, D. A., and P. W. Schmidt, Theoretical analysis of thermomagnetic properties, low-temperature hysteresis and domain structure of titanomagnetites, *Phys. Earth Planet. Inter., 30*, 300-316, 1982.

Conolly, J. R., and J. C. Ferm, Permo-Triassic sedimentation patterns, Sydney Basin, Australia, *Am. Assoc. Petr. Geol. Bull., 55*, 2018-2032, 1971.

Day, R., M. D. Fuller, and V. A. Schmidt, Hysteresis properties of titanomagnetites: Grain size and compositional dependence, *Phys. Earth Planet. Inter., 13*, 260-267, 1977.

Dunlop, D. J., Hysteretic properties of synthetic and natural monodomain grains, *Philos. Mag., 19*, 329-338, 1969.

Dunlop, D. J., and Ö. Özdemir, *Rock Magnetism: Fundamentals and Frontiers*, 573 pp., Cambridge Univ. Press, New York, 1997.

Dunlop, D. J., Ö. Özdemir, and P. W. Schmidt, Paleomagnetism and paleothermometry of the Sydney Basin, 2, Origin of anomalously high unblocking temperatures, *J. Geophys. Res.*, this issue.

Embleton, B. J. J., A review of the palaeomagnetism of Australia and Antarctica, *Paleoreconstruction of the Continents, Geodyn. Ser.*, vol. 2, edited by M. W. McElhinny and D. A. Valencio, pp. 77-92, AGU, Washington, D. C., 1981.

Embleton, B. J. J., and K. L. McDonnell, Magnetostratigraphy in the Sydney Basin, southeastern Australia, *J. Geomagn. Geoelectr., 32*, suppl. III, 1-10, 1980.

Enkin, R. J., and D. J. Dunlop, The demagnetization temperature necessary to remove viscous remanent magnetization, *Geophys. Res. Lett., 15*, 514-517, 1988.

Facer, R. A., and P. F. Carr, K-Ar dating of Permian and Tertiary igneous activity in the southeastern Sydney Basin, New South Wales, *J. Geol. Soc. Aust., 26*, 73-79, 1979.

Falvey, D. A., The development of continental margins in plate tectonic theory, *APEA J., 14*, 95-106, 1974.

Falvey, D. A., and M. F. Middleton, Passive continental margins: Evidence for a prebreakup deep crustal metamorphic subsidence mechanism, *Oceanol. Acta, 4*, 103-114, 1981.

Herbert, C., Depositional development of the Sydney Basin, *Geol. Surv. N.S.W. Bull., 26*, 10-52, 1980.

Idnurm, M., Late Mesozoic and Cenozoic palaeomagnetism of Australia, I, A redetermined apparent polar wander path, *Geophys. J. R. Astron. Soc., 83*, 399-418, 1985.

Irving, E., and L. G. Parry, The magnetism of some Permian rocks from New South Wales, *Geophys. J. R. Astron. Soc., 7*, 395-411, 1963.

Joplin, G. A., The shoshonite association: A review, *J. Geol. Soc. Aust., 15*, 275-294, 1968.

Kent, D. V., Thermoviscous remagnetization in some Appalachian limestones, *Geophys. Res. Lett., 12*, 805-808, 1985.

Kent, D. V., and N. D. Opdyke, Multicomponent magnetizations from the Mississippian Mauch Chunk formation of the central Appalachians and their tectonic implications, *J. Geophys. Res., 90*, 5371-5383, 1985.

Klootwijk, C., J. Giddings, and P. Percival, Palaeomagnetic reconnaissance of Upper Palaeozoic volcanics, northeastern Queensland, *Aust. Geol. Surv. Org. Rec., 1993/36*, 1993.

Lackie, M. A., The rock magnetism of granitic and ignimbritic rocks in the Lachlan and New England fold belts, N.S.W., Ph.D. thesis, Macquarie Univ., Sydney, Australia, 1989a.

Lackie, M. A., The palaeomagnetism and magnetic fabric of the Late Permian Dundee Rhyodacite, New England, *New England Orogen: Tectonics and Metallogenesis*, edited by J. D. Kleeman, Univ. of New England, Armidale, New South Wales, Australia, 1989b.

Lackie, M. A., D. H. French, and D. A. Clark, Magnetic mineralogy of felsic volcanics of the Conway-Bimurra area, northeast Queensland: Relationships to aeromagnetic anomalies and hydrothermal alteration, *CSIRO Div. Explor. Geosci. Restrict. Rep., 274R*, 1992.

Mayne, S. J., E. Nicholas, A. L. Bigg-Wither, J. S. Rasidi, and M. J. Raine, Geology of the Sydney Basin-A review, *Bull. Bur. Mineral. Res. Geol. Geophys. Aust., 149*, 229 pp., 1974.

McCabe, C., and R. D. Elmore, The occurrence and origin of Late Paleozoic remagnetization in the sedimentary rocks of North America, *Rev. Geophys., 27*, 471-494, 1989.

McElhinny, M. W., and J. Lock, IAGA paleomagnetic databases with Access, *Surv. Geophys., 17*, 575-591, 1996.

Middleton, M. F., and P. W. Schmidt, Paleothermometry of the Sydney Basin, *J. Geophys. Res., 87*, 5351-5359, 1982.

Moore, M. E., A. J. W. Gleadow, and J. F. Lovering, Thermal evolution of rifted continental margins: New evidence from fission tracks in basement apatites from southeastern Australia, *Earth Planet. Sci. Lett., 78*, 255-270, 1986.

Néel, L., Théorie du traînage magnétique des ferromagnétiques en grains fins avec applications aux terres cuites, *Ann. Géophys.*, *5*, 99-136, 1949.

Özdemir, Ö., and S. K. Banerjee, High temperature stability of maghemite, *Geophys. Res. Lett.*, *11*, 161-164, 1984.

Ozima, M., M. Ozima, and S. Akimoto, Low temperature characteristics of remanent magnetization of magnetite: Self-reversal and recovery phenomena of remanent magnetization, *J. Geomagn. Geoelectr.*, *16*, 165-177, 1964.

Packham, G. H. (Ed.), The geology of New South Wales, *J. Geol. Soc. Aust.*, *16*, 654, 1969.

Pullaiah, G., E. Irving, K. L. Buchan, and D. J. Dunlop, Magnetization changes caused by burial and uplift, *Earth Planet. Sci. Lett.*, *28*, 133-143, 1975.

Raam, A., Petrology and diagenesis of Broughton Sandstone (Permian), Kiama District, New South Wales, *J. Sediment. Petrol.*, *38*, 319-331, 1968.

Robertson, W. A., Palaeomagnetic results from some Sydney Basin igneous rock deposits, *J. Proc. R. Soc. N.S.W.*, *112*, 31-35, 1979.

Robertson, W. A., and L. Hastie, A palaeomagnetic study of the Cygnet Alkaline Complex of Tasmania, *J. Geol. Soc. Aust.*, *8*, 259-268, 1962.

Schmidt, P. W., A new palaeomagnetic investigation of Mesozoic igneous rocks in Australia, *Tectonophysics*, *33*, 1-13, 1976a.

Schmidt, P. W., The non-uniqueness of the Australian Mesozoic palaeomagnetic pole position, *Geophys. J. R. Astron. Soc.*, *47*, 285-300, 1976b.

Schmidt, P. W., The Late Palaeozoic and Mesozoic palaeomagnetism of Australia, Ph.D. thesis, Aust. Natl. Univ., Canberra, 1976c.

Schmidt, P. W., and B. J. J. Embleton, Magnetic overprinting in southeastern Australia and the thermal history of its rifted margin, *J. Geophys. Res.*, *86*, 3998-4008, 1981.

Schmidt, P. W., and I. McDougall, Palaeomagnetic and potassium-argon dating studies of the Tasmanian dolerites, *J. Geol. Soc. Aust.*, *25*, 321-328, 1977.

Walton, D., Time-temperature relations in the magnetization of assemblies of single domain grains, *Nature*, *286*, 245-247, 1980.

Wellman, P., and I. McDougall, Potassium-argon ages on the Cainozoic volcanic rocks of New South Wales, *J. Geol. Soc. Aust.*, *21*, 247-272, 1974.

Xu, S., and D. J. Dunlop, The theory of partial thermoremanent magnetization in multidomain grains, 2, Effect of microcoercivity distribution and comparison with experiment, *J. Geophys. Res.*, *99*, 9025-9033, 1994.

D. A. Clark and P. W. Schmidt, Division of Exploration and Mining, CSIRO, North Ryde, New South Wales 2113, Australia. (e-mail: phils@ syd.deg.csiro.au)

D. J. Dunlop and Ö. Özdemir, Department of Physics, Erindale College, University of Toronto, 3359 Mississauga Road North, Mississauga, Ontario, Canada L5L 1C6. (e-mail: dunlop@physics.utoronto.ca)

(Received January 16, 1997; revised July 7, 1997;
accepted August 27, 1997.)